SOME NUMERICAL URBAN BOUNDARY-LAYER STUDIES

ZBIGNIEW SORBJAN* and MAREK ULIASZ

Institute of Environmental Engineering, Technical University of Warsaw, Poland

(Received in final form 7 December, 1981)

Abstract. Two types of models, describing respectively the thermal and the dynamic structure of the urban boundary layer are presented. The influence of density and height of urban buildings, urban traffic, man-made heat flux, changes of albedo and existence of an aerosol layer are tested. The models give a possibility of explaining the influence of selected factors on the atmospheric state over an urban area.

1. Introduction

The physical state of the atmosphere undergoes considerable modification over an urban area. This general phenomenon has been the subject of an increasing number of studies during recent years, including full-scale studies, numerical modelling and physical modelling; see, e.g., Oke (1974) and Högström (1978) for comprehensive reviews. In spite of this there is still considerable uncertainty as to the relative role of the various factors in creating the observed phenomena.

In the present paper a numerical modelling approach has been applied. Various factors known or suspected to influence the urban atmospheric structure have been included in three numerical models: a simple thermal model, a one-dimensional dynamical model and a three-dimensional dynamical model. All the models are steady state and represent a more or less idealized urban situation, in order to elucidate the impact of each of a number of well defined physical factors on the state of the urban atmosphere.

2. Numerical Simulation of the Thermal Structure of an Urban Boundary Layer

Numerous research results indicate that the air temperature at least during night-time conditions over urban areas is higher than in the rural environs (Chandler, 1976; Clarke and McElroy, 1970; Landsberg, 1956; Oke, 1974; Oke and Maxwell, 1975; Oke and Hannell, 1970). This phenomenon, usually defined as an 'urban heat island', is due to many factors, such as artificial heat generation within urban areas, attenuating short-wave solar radiation, long-wave radiation of atmospheric and terrestrial origin, trapping of heat due to obstruction of air flow in the surface layer, difference in heat capacity of urban and rural fabric as well as vertical redistribution of heat by increased turbulence.

To evaluate man-made temperature changes in urban areas, a simple two-dimensional model has been introduced (Sorbjan, 1978b). The model is based on the two-dimensional thermal equation:

$$U_0 \frac{\partial T'}{\partial x} = K_0 \frac{\partial^2 T'}{\partial z^2} - \frac{1}{c_p \rho_0} \frac{\partial R'}{\partial z} \tag{1}$$

* On sabbatical at Meteorological Department, University Uppsala, Sweden.

Boundary-Layer Meteorology **22** (1982) 481–502. 0006–8314/82/0224–0481$03.30.

with boundary conditions for $z = 0$:

$$K_0 c_p \rho_0 \frac{\partial T'}{\partial z} = [S(1-a) - F^{\uparrow} + F^{\downarrow}] - [S_0(1-a_0) - F_0^{\uparrow} + F_0^{\downarrow}] + Q_s ,$$

for $z = H$: $T' = 0$,
for $x = 0$: $T' = 0$,
where

U = wind velocity,
T = temperature,
K_0 = thermal eddy diffusivity coefficient,
c_p = specific heat at constant pressure,
ρ = air density,
R = $F^{\uparrow} - F^{\downarrow} - S$ = effective radiative heat flux,
a = albedo,
S = flux of short-wave radiation,
$F^{\uparrow}, F^{\downarrow}$ = fluxes of long-wave upward and downward radiation, respectively,
Q_s = anthropogenic heat flux,
H = height of the boundary layer.

Primes signify differences between urban and rural values, subscripts '0' signify rural undisturbed values. The model was used to investigate the influences of three important factors of the formation of urban heat islands, i.e.,
- influence of anthropogenic heat generation,
- influence of albedo changes, and
- influence of urban aerosols.

Differences of latent heat and surface soil fluxes in urban and rural areas were not taken into consideration. Energy partitioning (e.g., Oke, 1978) shows that these differences are of the same order as another terms in the surface heat balance, used as the boundary condition for Equation (1).

The thermal eddy diffusivity coefficient was assumed constant, which implies that diurnal changes of turbulent intensity are not taken into consideration. We also assumed, for simplification, a horizontally constant urban wind velocity profile.

Short- and long-wave radiative fluxes in rural and polluted urban areas were obtained using the scheme worked out by Atwater and described in Appendix C derived from Pandolfo and Jacobs (1973). The scheme employs the integrated form of Schwarzschild's equations to compute absorption and emission of radiation in the infrared spectrum, and uses the integrated form of Beer's law to compute absorption and scattering of solar radiation. It is assumed that long-wave radiation is absorbed by water vapour (an amount of 2.5 cm precipitated water) and carbon dioxide (0.0311% by volume) in the free atmosphere and by aerosols in the boundary layer. Short-wave radiation is scattered and absorbed by aerosols in the boundary layer, and by gases such as oxygen and ozone in the free atmosphere; short-wave radiation is absorbed by water vapour in the free atmosphere. The infrared transmission function for water vapour, carbon dioxide, and

the solar spectrum transmission function for gases and water vapour are taken from papers cited in Pandolfo and Jacobs (1973). The transmission functions for infrared aerosol absorption and solar radiation aerosol absorption were worked out by Atwater (1971) using the Mie series and assuming a modified gamma distribution to represent the aerosol size distribution (modal radius: 0.005 μ and concentration of particles: $N = 10^5\ \mathrm{cm}^{-3}$). The infrared transmission function for aerosols is spectrally averaged and the solar function assumes a wavelength of 0.485 μ.

The aerosol absorption and scattering coefficients for solar radiation B_a^s, B_s^s, and the infrared absorption coefficient B_a^L were chosen from Atwater's tables (Atwater, 1971). The values are $B_a^s = 0.0230\ \mathrm{km}^{-1}$, $B_s^s = 0.1184\ \mathrm{km}^{-1}$, $B_a^L - 0.0120\ \mathrm{km}^{-1}$, for aerosol with complex refraction index $m = 1.2 - \alpha i$, where $\alpha = 0.1$ for solar radiation, and 0.25 for infrared radiation, $i = \sqrt{-1}$, and concentration $N_0 = 10^5\ \mathrm{cm}^{-1}$. For other values of N the coefficients B should be multiplied by the factor N/N_0.

The total transmission function for infrared radiation is assumed to be the product of transmission by gases and the transmission by aerosols. Gaseous transmission is the sum of the transmission due to water vapour and due to carbon dioxide. The total transmission in the solar spectrum is the product of the individual transmission functions for gases, water vapour and aerosols. Calculations were conducted for $\cos Z = 0.6157$ during day-time, where Z is zenith angle, and for clear skies.

In the model, the following additional assumptions were made:

(a) Anthropogenic heat flux was defined as a parabolic function of the urban fetch:

$$Q_s(x) = 4Q_{s,\,max}\,\frac{x(L-x)}{L^2} \tag{3}$$

where L is a characteristic width of the urban area.

(b) Urban aerosol concentration was defined as:

$$N(x, z) = 4N_{\max}\,\frac{x(L-x)}{L^2}\,I(h_1, h_2) \tag{4}$$

$$\text{where } I(h_1, h_2) = \begin{cases} 1 & \text{for } h_1 < z < h_2\,, \\ 0 & \text{otherwise.} \end{cases}$$

From Equation (4), it follows that the concentration in the aerosol layer is vertically uniform, in agreement, e.g., with measurements of De Luisi (1967). A horizontal parabolic distribution is very simplified and does not take into consideration aerosol advection downwind of the urban area.

(c) The albedo in the urban area was defined as:

$$a(x) = 4(a_{\max} - a_0)\,\frac{x(L-x)}{L^2} + a_0 \tag{5}$$

where $Q_{s,\max}$, $N_{\max}$, $a_{\max}$ are maximum values of parameters in the urban area, h_1, h_2 are boundaries of the urban aerosol layer.

(d) The wind velocity profile was defined as

$$U_0 = G\left(\frac{z}{H}\right)^{0.3} \tag{6}$$

where G = geostrophic wind velocity.

Equation (2) was solved numerically for the following values of the parameters: $a_0 = 0.20$, $a_{\max} = 0.15$, $N_{\max} = 10^4$; 10^5; $10^6\ \mathrm{cm}^{-3}$, $K_0 = 10\ \mathrm{m}^2\ \mathrm{s}^{-1}$, $Q_{s,\max} = 100.0\ \mathrm{W\ m}^{-2}$, $G = 10\ \mathrm{m\ s}^{-1}$, $L = 20$ km, $H = 1500$ m.

First of all let us discuss the impact of aerosols on the structure of the UBL. Figures 1–3 show urban–rural temperature difference isolines, obtained from the model for daytime conditions and for different aerosol concentrations $N_{\max} = 10^4$, 10^5, $10^6\ \mathrm{cm}^{-3}$. According to Atwater (1971), a typical urban value for N is $10^5\ \mathrm{cm}^{-3}$. Anthropogenic heat flux was set at zero.

It can be seen from the figures that the heat island intensity decreases when aerosol concentrations increase. For $N_{\max} = 10^4\ \mathrm{cm}^{-3}$, an urban heat island with maximum surface contrast of + 0.39 K is obtained because of albedo reduction in the urban area. For $N_{\max} = 10^5$, $10^6\ \mathrm{cm}^{-3}$ in spite of the albedo reduction, radiation extinction in the aerosol layer induces an urban cold island. In the three cases discussed, the ratios of short-wave radiation fluxes S, S_0 for the urban and rural surfaces are, respectively,

$$\frac{S}{S_0} = 99.1\%;\ 91{,}3\%;\ 47.3\%\ .$$

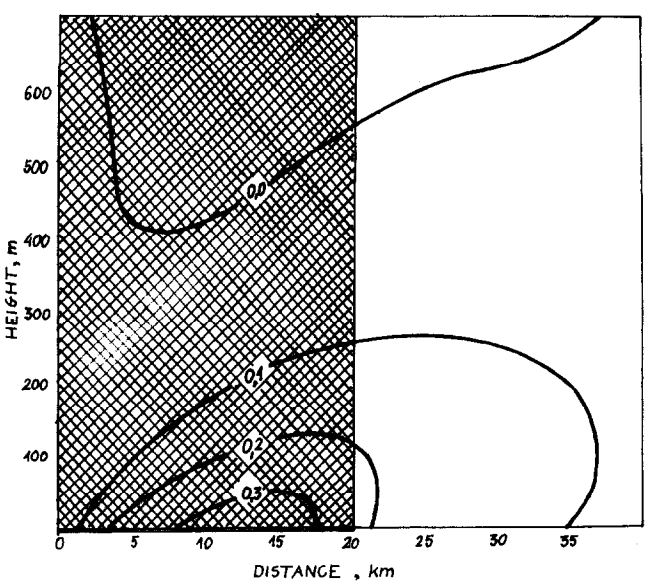

Fig. 1. Urban-rural temperature deviations isolines (K) in numerical experiment No. 1 (aerosol and albedo influences during day-time, $N_{\max} = 10^4\ \mathrm{cm}^{-3}$). Aerosol layer is shaded.

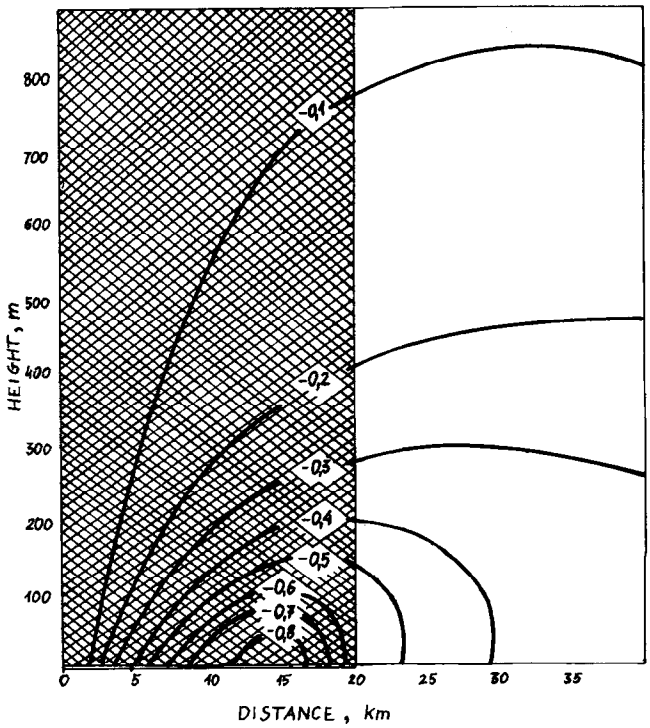

Fig. 2. Urban-rural temperature deviation isolines (K) in numerical experiment No. 2 (aerosol and albedo influences during day-time, $N_{max} = 10^5$ cm^{-3}).

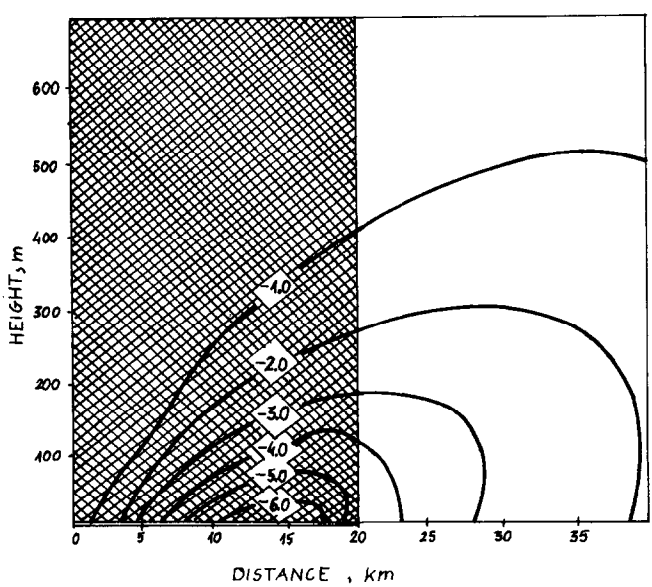

Fig. 3. Urban-rural temperature deviation isolines (K) in numerical experiment No. 3 (aerosol and albedo influences during day-time, $N_{max} = 10^6$ cm^{-3}).

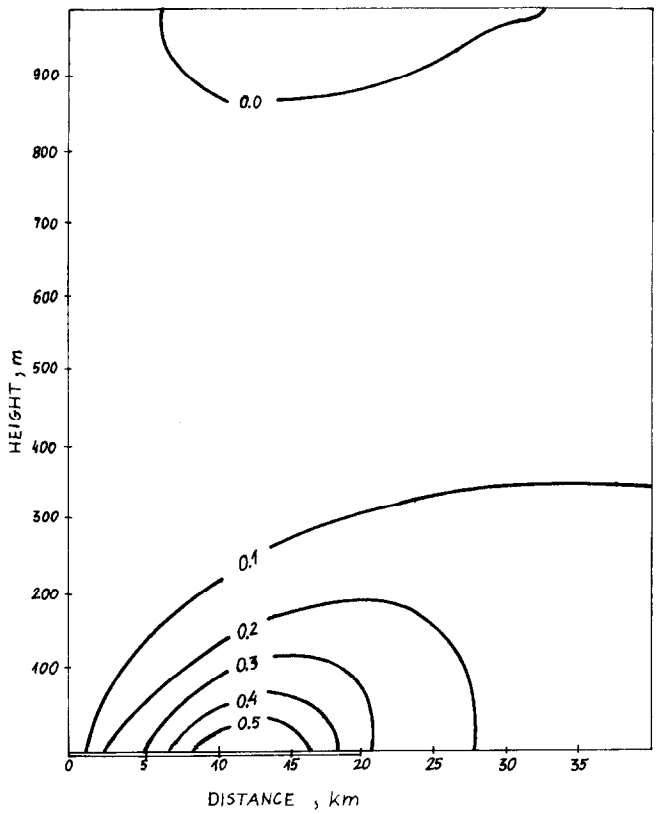

Fig. 4. Urban-rural temperature deviation isolines (K) in numerical experiment No. 4 (albedo influence only, $N_{max} = 0$).

Urban temperature rises caused only by albedo changes are shown in Figure 4. The maximum heat island effect is 0.54 K. The ratio of urban to rural energies absorbed by the surface equals 104% in this case.

Anthropogenic heat flux is one of the most important factors inducing urban heat island formation for many towns. As shown in Figure 5, for anthropogenic heat flux $Q_s = 100.0$ W m^{-2}, the maximum temperature deviation at night was 1.66 K (for day-time 2.2 K). When the anthropogenic heat flux is set to zero at night and the layer of aerosols ($N_{max} = 10^5$ cm^{-3}) is taken into consideration, a maximum temperature deviation of 0.31 K was obtained (Figure 6).

Numerical experiments showed that heat island intensity decreased when wind-speed increased. The vertical extent of the heat island (defined by the 0.1 K isoline) induced by anthropogenic heat flux with an aerosol layer present amounts to 250 m in the day-time and 600 m at night. The day-time mixing height in urban heat islands can change for different values of thermal diffusivity K_0. However, that effect was not investigated in our study.

Although our model emphasis the effects of radiative transfer and anthropogenic heat generation and simplifies other effects, the results obtained are in qualitative agreement with results of measurements in urban areas described in Oke's review (Oke, 1974).

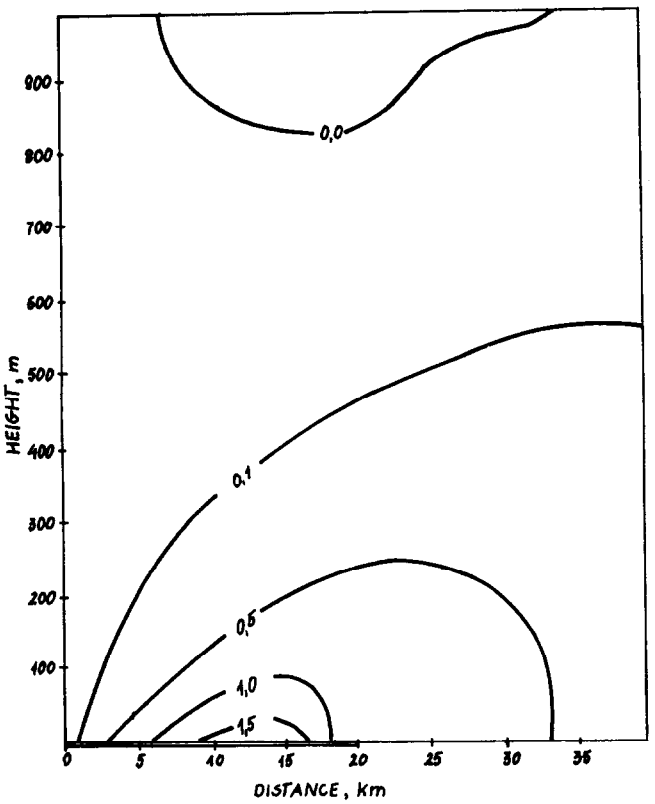

Fig. 5. Urban-rural temperature deviation isolines (K) in numerical experiment No. 5 (anthropogenic heat flux influence during night-time).

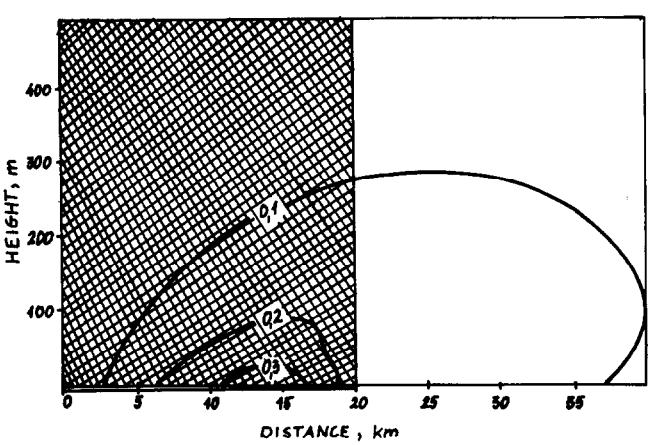

Fig. 6. Urban-rural temperature deviation isolines (K) in numerical experiment No. 6 (aerosol influence during night-time, $N_{max} = 10^5$ cm^{-3}, $Q_s = 0$).

TABLE I

Characteristics of numerical experiments

No.	N_{max} [cm^{-3}]	Aerosol layer		$Q_{s,max}$ [W m^{-2}]	G [m s^{-1}]	Heat balance at the earth surface [W m^{-2}]			
		h_1 [m]	h_2 [m]			S	$F\downarrow$	$F\uparrow$	$B = S(1-a) + F^{\downarrow} - F^{\uparrow}$
1	10^4	10	1000	0	10	649.0	323.6	423.8	439.2
2	10^5	10	1000	0	10	598.3	322.6	419.5	339.9
3	10^6	10	1000	0	10	309.7	322.0	398.1	177.6
4	0	–	–	0	10	655.0	323.8	424.3	433.9
5	0	–	–	100	10	0.0	325.5	428.3	–40.3
6	10^5	10	1000	0	10	0.0	333.7	423.5	–89.8

Table I (continued)

No.	Ratio of urban and rural surface balance terms [%]				Ratio of urban and rural energy absorbed by surface [%]	$\max_x T(0,x)$ [°C]	Reference to figure
	S/S_0	$F^{\downarrow}/F_0^{\downarrow}$	$F^{\uparrow}/F_0^{\uparrow}$	B/B_0			
1	99.1	102.2	100.3	103.5	103.1	0.39	1
2	91.3	99.9	99.4	80.1	95.0	−0.86	2
3	47.3	99.7	94.2	41.8	49.2	−7.28	3
4	100.0	100.3	100.4	104.6	104.0	0.54	4
5	–	100.8	101.4	40.5	–	1.66	5
6	–	103.9	100.3	90.3	–	0.31	6

3. Numerical Simulation of the Dynamical Structure of an Urban Boundary Layer

In this section an attempt is made to explain the influence of urban buildings, urban traffic and the urban heat island on the dynamical structure of the UBL. The dynamics of the three-dimensional UBL under the assumption of steady-state, hydrostatic and incompressible flow can be described by the following set of equations:

$$u\frac{\partial \mathbf{V}}{\partial x} + v\frac{\partial \mathbf{V}}{\partial y} + w\frac{\partial \mathbf{V}}{\partial z} = \frac{\partial}{\partial z}K\frac{\partial \mathbf{V}}{\partial z} - f\mathbf{k}\times(\mathbf{V}-G) - c_r|\mathbf{V}|\mathbf{V}I_h + \\ + \int_z^H \operatorname{grad}\theta'\,\mathrm{d}z\,, \tag{7}$$

$$u\frac{\partial \theta'}{\partial x} + v\frac{\partial \theta'}{\partial y} + w\frac{\partial \theta'}{\partial z} = \frac{\partial}{\partial z}K\frac{\partial \theta'}{\partial z}\,, \tag{8}$$

$$\frac{\partial w}{\partial z} = -\left(\frac{\partial u}{\partial x} + \frac{\partial v}{\partial y}\right), \tag{9}$$

$$K = \sqrt[3]{1^6\left(\left|\frac{\partial \mathbf{V}}{\partial z}\right|^2 - \beta \frac{\partial \theta}{\partial z} I_\theta\right)^{1.5} + 1^4 E}, \tag{10}$$

$$1 = \frac{\kappa z}{1 + \dfrac{\kappa z f}{0.000\,27\,|\mathbf{G}|\, s}}, \tag{11}$$

$$s = \begin{cases} \left(100.0 \dfrac{\partial \theta}{\partial z} + 1.0\right)^{-1} & \text{for } \dfrac{\partial \theta}{\partial z} > 0, \\ \left(7.9 \left|\dfrac{\partial \theta}{\partial z}\right|^{0.25} + 1.0\right), & \text{for } \dfrac{\partial \theta}{\partial z} < 0, \end{cases} \tag{12}$$

$$I_h = \begin{cases} 1, & \text{for } z < b_b, \\ 0, & \text{for } z > h_b, \end{cases} \tag{13}$$

$$I_\theta = \begin{cases} 1, & \text{for } \dfrac{\partial \theta}{\partial z} < 0, \\ 0, & \text{for } \dfrac{\partial \theta}{\partial z} > 0, \end{cases} \tag{14}$$

with boundary conditions as follows:

$$\text{for } z = z_0,\ \mathbf{V} = 0,\ w = 0,\ \theta' = \theta'_s(x, y) \tag{15}$$

$$\text{for } z = H,\ \mathbf{V} = \mathbf{G},\ \theta' = 0, \tag{16}$$

$$\text{for } x = 0,\ \mathbf{V} = \mathbf{V}_0(z),\ \theta' = 0, \tag{17}$$

$$\text{for } y = 0,\ \mathbf{V} = \mathbf{V}_0(z),\ \theta' = 0, \tag{18}$$

where

c_r = urban resistance coefficient,
E = rate of the turbulent energy generation,
f = Coriolis parameter,
$\mathbf{G}$ = geostrophic wind vector,
h_b = mean height of buildings,
$\mathbf{k}$ = z axis vector,
l = mixing length,
$\mathbf{V}$ = horizontal wind vector, $\mathbf{V} = (u, v)$,
w = vertical velocity,
x, y, z = Cartesian coordinates,

β = buoyancy parameter, $\beta = g/\overline{T}$,

κ = von Karman constant,

θ = potential temperature,

z_0 = rural roughness parameter (we assume that urban roughness is introduced to the model by terms proportional to c_r; if $c_r = 0$, the model describes the flow over the rural area with the roughness length z_0).

The remaining symbols and the meaning of primes and subscripts were given in the previous section. In the above equations the x-axis is assumed to be the direction of the geostrophic wind vector.

We have assumed (cf. Appendix A) that the turbulent energy generation in the urban area can be expressed in the form:

$$E = E_b + E_c \tag{19}$$

where the turbulent energy generation resulting from urban building resistance E_b can be defined as

$$E_b = c_r |\mathbf{V}|^3 I_h \tag{20}$$

and the turbulent energy generation resulting from urban traffic E_c can be described as

$$E_c = c_s W^3 I_s, \qquad I_s = \begin{cases} 1. & \text{for } z < h_s \\ 0. & \text{for } z > h_s \end{cases} \tag{21}$$

where c_s is a coefficient, W is the mean speed of cars and h_s is the height of cars.

As shown in Appendix A, the coefficient c_r is expected to attain values in the range 10^{-3} to 10^{-2} m^{-1}, and the values of E_c to vary from 10^{-3} to 1 m^2 s^{-3}.

Equation (7) is the vector form of the equations of motion for stationary flow. The third term on the right-hand side of this equation describes the loss of momentum caused by resistance of urban buildings and the last term on this side is connected to pressure perturbation over the urban area due to thermal nonhomogeneity. In the temperature differences Equation (8), we neglected radiation effects and assumed for simplification neutral atmospheric stability above the rural area. The form of the continuity Equation (9) for incompressible flow is used in the model. Equation (10) was obtained from the turbulent energy equation in which the turbulent energy diffusion term had been neglected and additional turbulent energy generation E in the urban area had been added (see Appendix B). The mixing length was defined by the modified Blackadar formula (Blackadar, 1962), by using the stability function s. The stability function s was formulated as in Sharon (1965).

The finite-difference scheme used to solve the model equations is analogous to the scheme applied by Estoque and Bhumralhar (1970). Grid points along the vertical axis were located at the levels z_i, $i = 1, 2, \ldots, 15$, which fulfil the equation $\zeta_i = z_i + a \ln z_i/z_0$, where $\zeta_i = (i-1)\Delta\zeta + z_0$, $z_0 = 0.1$ m; the constants $\Delta\zeta$ and a were found from the condition that $z_8 = 100$, $z_{15} = 1500$ m. Introduced in that way, log-linear spacing guarantees proper accuracy close to the ground (Taylor and Delage, 1971). The grid points along horizontal axes correspond to the distances 0, 2, 4, 5, 6, 8, 10, 13, 17 km.

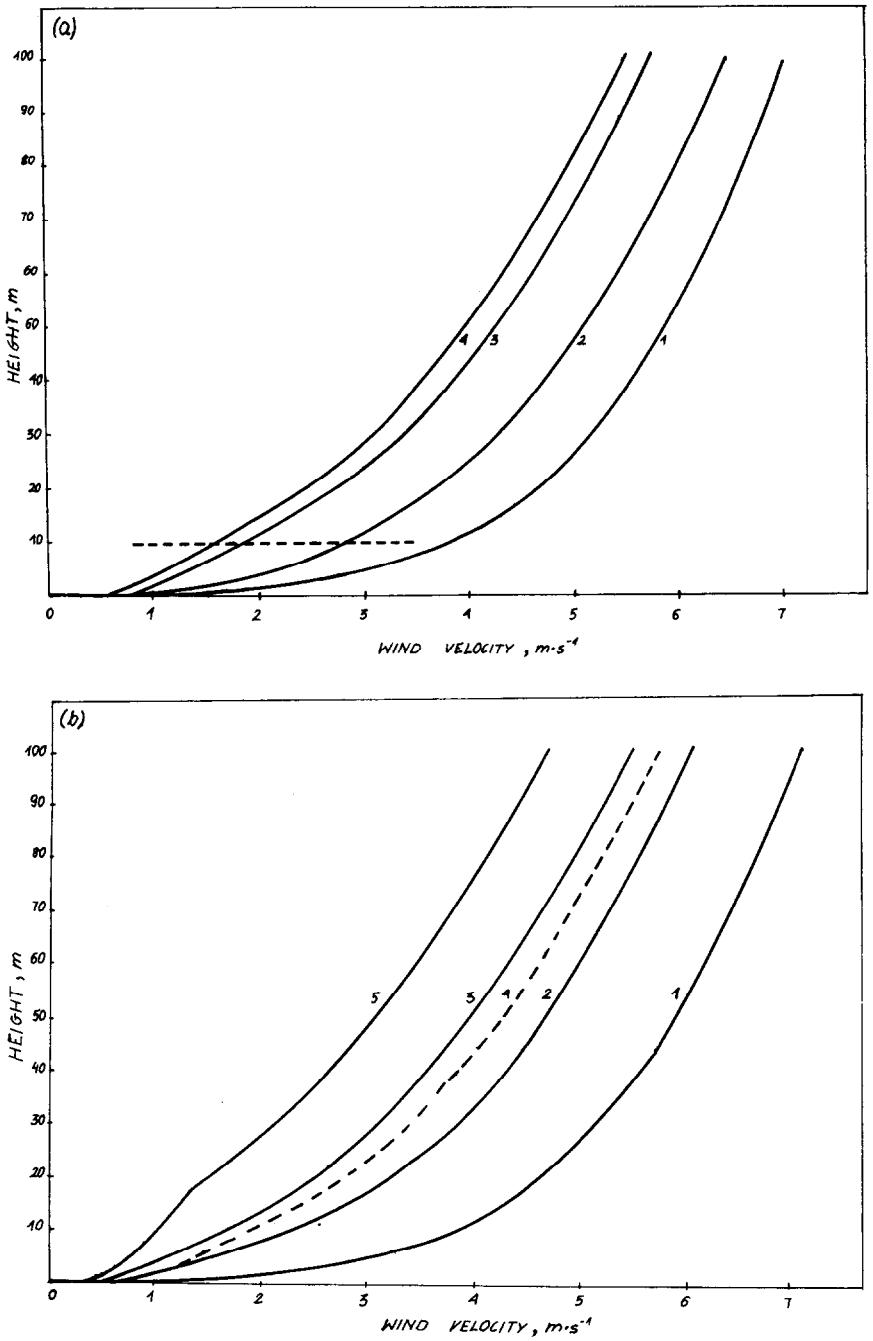

Fig. 7. Vertical wind distributions in urban surface layer in neutral conditions, (G = 10 m s^{-1}), for different values of the urban resistance coefficient c_r and of height of buildings h_b (one-dimensional version of dynamic model): (a) 1. $c_r = 0$; 2. $c_r = 0.001$ m^{-1}; 3. $c_r = 0.005$ m^{-1}; 4. $c_r = 0.010$ m^{-1} (h_b = 10 m); (b) 1. $c_r = 0$, $h_b = 0$; 2. $c_r = 0.010$ m^{-1}, h_b = 5.6 m; 3. $c_r = 0.010$ m^{-1}, h_b = 10 m; 4. $c_r = 0.005$ m^{-1}, h_b = 10 m; 5. $c_r = 0.010$ m^{-1}, h_b = 18 m.

Assuming horizontal homogeneity first, some numerical experiments were carried out with a one-dimensional version of the model for different values of the resistance coefficient c_r, height of buildings and turbulent energy generation due to urban traffic (Sorbjan, 1978a).

Figure 7 shows the characteristic decrease of wind velocity in an urban area resulting from building resistance. Vertical distributions of wind for different values of both c_r and h_b are similar. For $c_r = 10^{-2}\ \mathrm{m}^{-1}$, $h_b = 10$ m, the wind velocity at a height of 100 m above the city may be reduced by 35%. Distributions of the turbulence coefficient for neutral rural and urban conditions, obtained from the model, are presented in Figure 8. In both cases the coefficient K reaches its highest value at a height of 100 m. For $c_r = 10^{-2}\ \mathrm{m}^{-1}$,

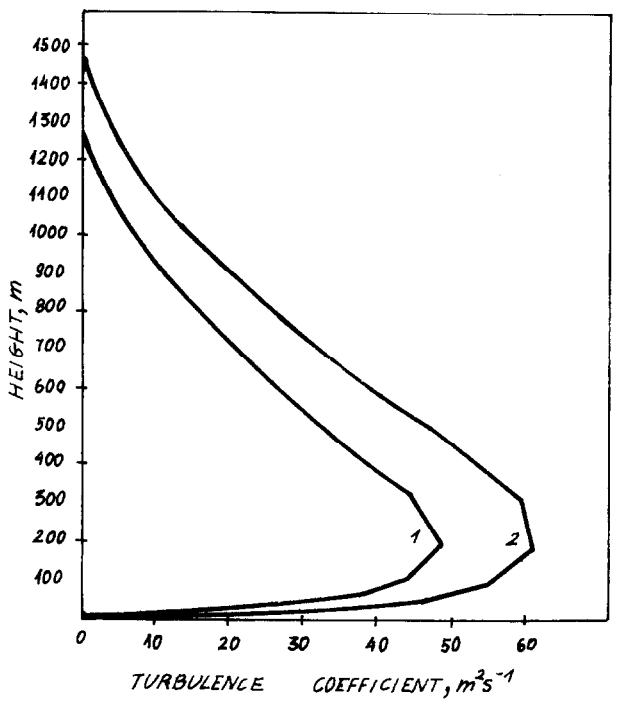

Fig. 8. Vertical distribution of the turbulence coefficient for neutral conditions ($G = 10$ m, $c_r = 0.01\ \mathrm{m}^{-1}$, $h_b = 10$ m). (1) rural area, (2) urban area.

$h_b = 10$ m, the urban maximum value of the turbulence coefficient is about 30% greater than the maximum value reached outside of cities. The function K reaches a value close to zero about 200 m higher in urban areas than it does in rural areas. This implies that the height of the boundary layer is greater in urban areas than in the surrounding rural areas.

Modifications of wind velocity and of the turbulence coefficient for different values of the turbulent energy generation due to traffic E_c are shown in Figure 9. The influence of traffic is greatest in the urban building layer. The wind velocity in this layer can be about half as large (for $E_c = 1\ \mathrm{m}^2\ \mathrm{s}^{-3}$) as the velocity obtained from the model in which

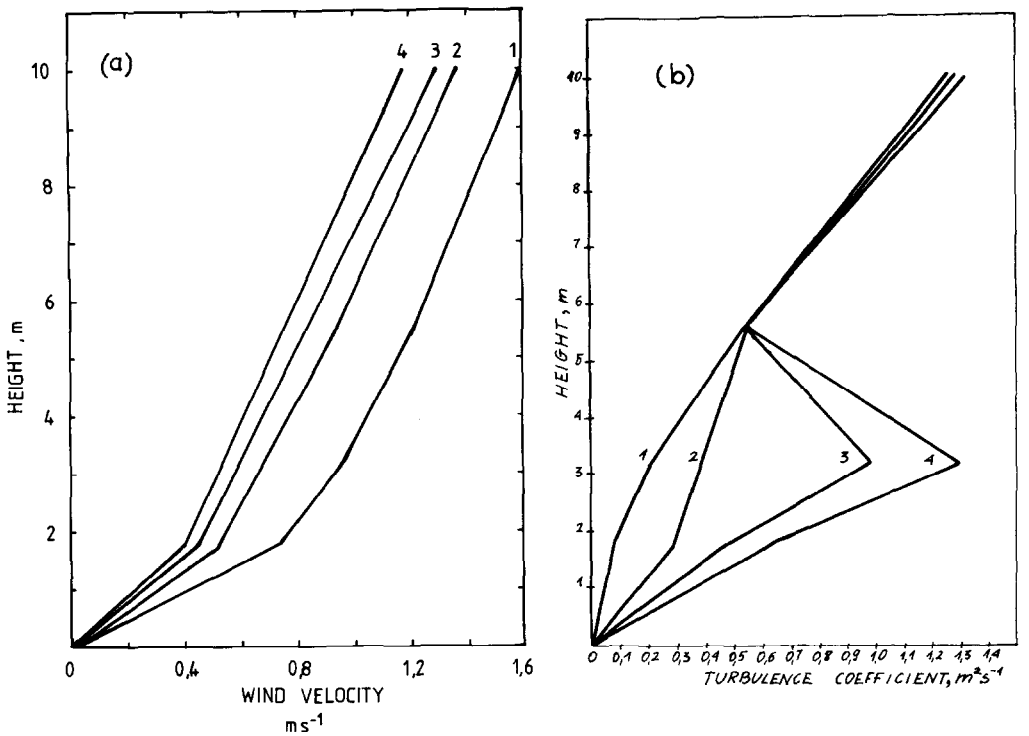

Fig. 9. Traffic influence on (a) the wind distribution and on (b) the turbulence coefficient distribution in the building layer ($c_r = 0.01\ m^{-1}$, $h_b = 10$ m, neutral conditions); 1. $E_s = 0$; 2. $E_s = 0.1\ m^2\ s^{-3}$; 3. $E_s = 0.5\ m^2\ s^{-3}$; 4. $E_s = 1\ m^2\ s^{-3}$.

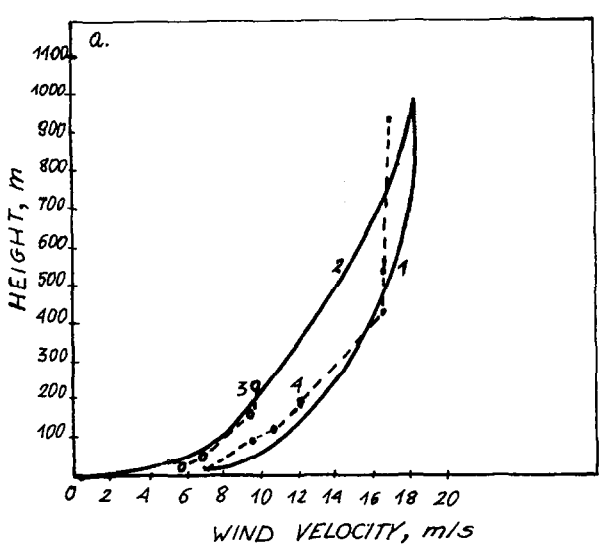

Fig. 10. Comparison of the wind profiles obtained from the model for urban area (1) and for rural area (2) together with data for Leningrad (3) and Voeykovo (4) by Lazareva *et al.* (1975), for neutral conditions.

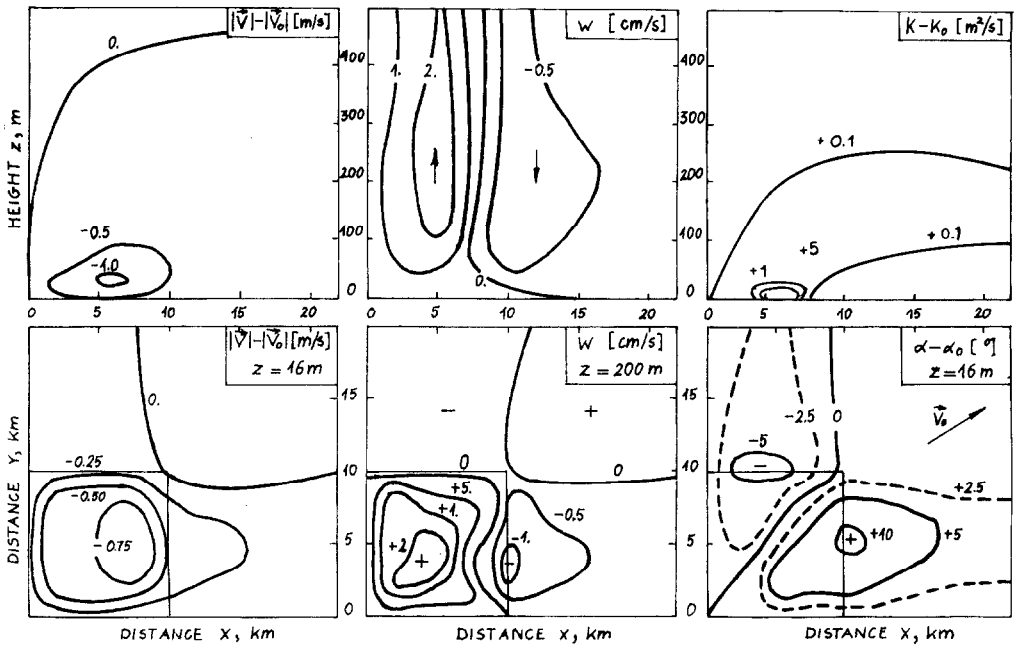

Fig. 11a.

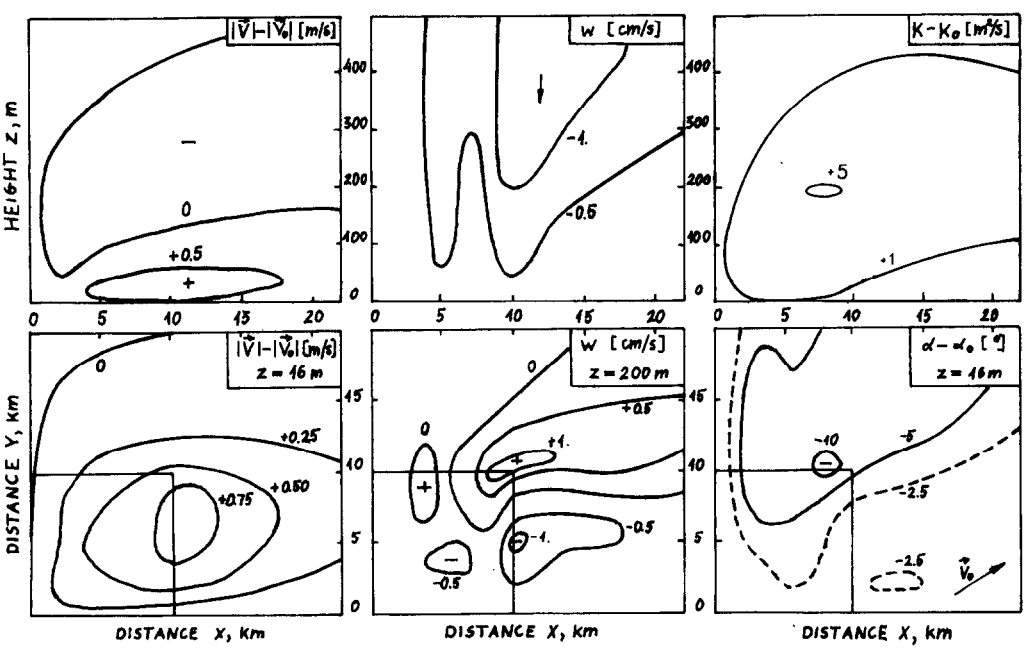

Fig. 11b.

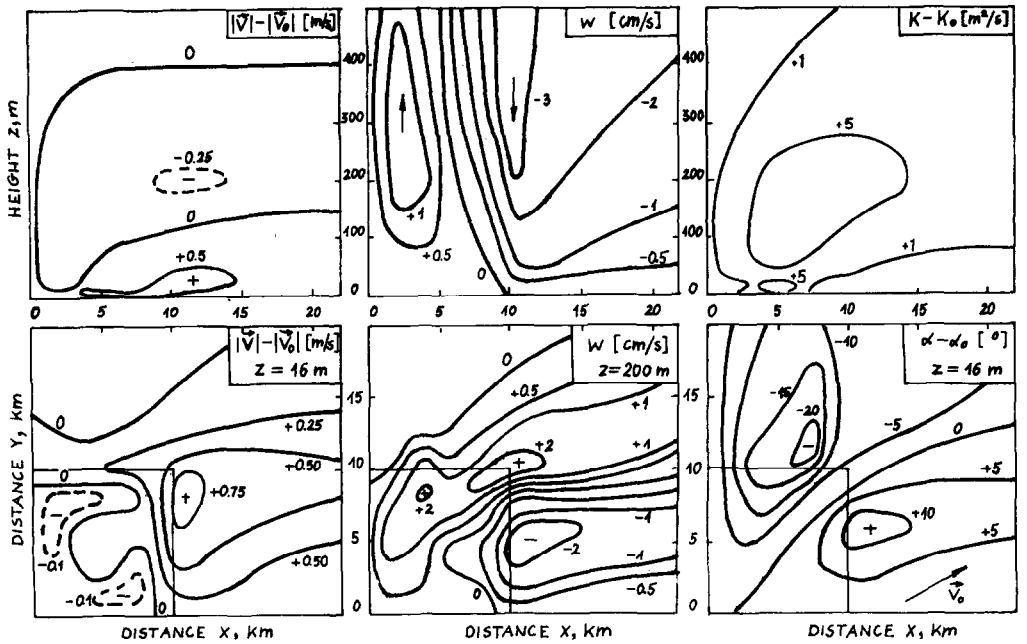

Fig. 11c. Perturbation of flow in the UBL for geostrophic wind velocity, $G = 5$ m s^{-1} (above – at xz plane for $y = 5$ km, below – at xy plane): (a) the effect of buildings ($h_b \neq 0$, $\theta' = 0$); (b) the effect of the urban heat island ($h_b = 0$, $\theta' \neq 0$); (c) the effect of buildings and the heat island ($h_b \neq 0$, $\theta' \neq 0$).

traffic was not considered at all. The changes of the turbulence coefficient are greatest in the layer where there are moving vehicles. In this layer the values of the turbulence coefficient may be 6 times greater than that obtained from the model in which traffic is not considered.

The comparison of wind profiles obtained from the one-dimensional model and the observed wind distribution given by Lazareva *et al.* (1975) is presented in Figure 10. This figure demonstrates good agreement between the measured wind profiles in urban and rural conditions and the wind distribution obtained from the model for a resistance coefficient $c_r = 0.01$ m^{-1} and for a mean height of buildings $h_b = 10$ m.

In order to study the influence of urban buildings and the urban heat island on the perturbation of flow in the UBL, some numerical experiments were carried out with a three-dimensional version of the model of an 'idealized city' in the form of a square with a 10 km side (Uliasz, 1979). We have assumed that the height of buildings – h_b, the urban resistance coefficient – c_r and the urban-rural temperature difference – θ_s' all increase from 0 at the edge of the city to maximum values in the centre. These maximum values for h_b, c_r, and θ_s' are equal to 16 m, 0.2 m^{-1} and 5 K, respectively. We studied the dynamics of the UBL for different geostrophic wind velocities separately for the effect of urban buildings and for the effect of urban heat island and for both effects together.

The urban buildings in the case of $\theta_s' = 0$ cause a decrease of wind velocity over the urban area associated with upward motions (Figure 11a). On the lee side of the city, an

area with downward motions occurs. The wind direction perturbations are shown by changes of angle α between wind direction at height $z = 16$ m and the direction of the geostrophic wind. A positive value of the urban-rural differences of this angle $(\alpha - \alpha_0)$ means cyclonic change of wind direction in the UBL. The perturbations of wind direction due to the urban buildings decrease with the growth of the wind velocity.

For a smooth city, i.e., $h_b = 0$, but with $\theta_s' \neq 0$, the windspeed over the city increases (Figure 11b). Two phenomena causing the increase of windspeed in the smooth and heated UBL are: (1) additional pressure gradient directed inward to the centre of the heat island; and (2) increase of vertical momentum exchange above the city. On the lee side of the city, where the growth of wind velocity is the greatest, downward motions occur with associated upward motions. An increase of geostrophic wind velocity causes an increase of downward velocities and a decrease of upward velocities. Above a layer with increased wind velocity, a small decrease of horizontal velocity occurs.

On the basis of the above results, we conclude that the roughness effect and the heat island effect tend to influence the urban wind field in opposite directions.

The most intensive growth of turbulence due to urban buildings takes place in the layer up to the height of about 20 m. The urban heat island generates an area of increased turbulence above the city and in its lee up to a height of about 200 m.

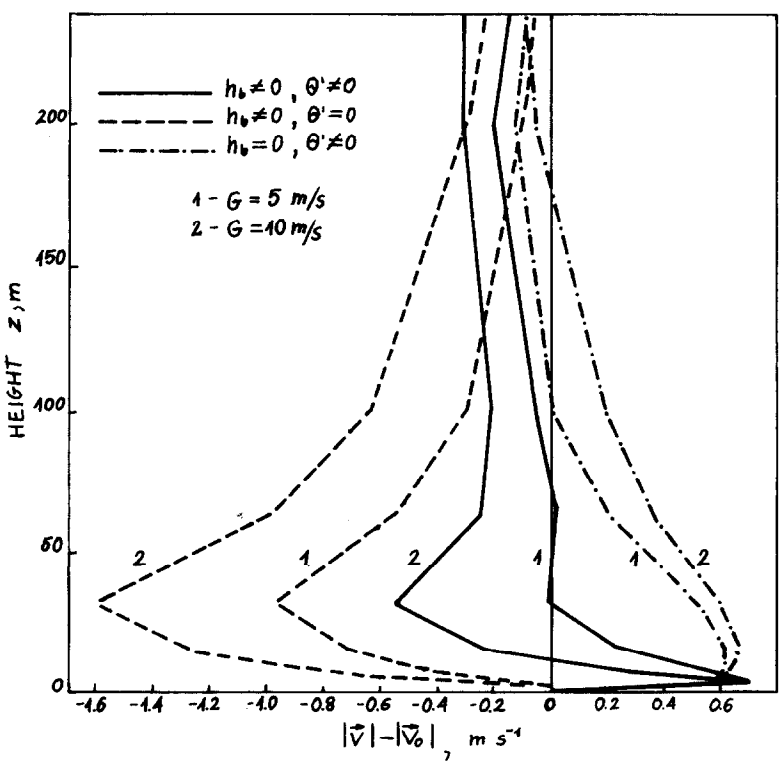

Fig. 12. Perturbation of wind velocity above centre of city ($x = y = 5$ km).

The perturbations of flow in the UBL connected with simultaneous influence of urban buildings and an urban heat island are more complex (Figure 11c) being dependent on the geostrophic wind velocity. Figure 12 presents the vertical distribution of urban-rural wind velocity differences for two geostrophic wind values. Variations of wind velocity due to the urban heat island depend very slightly on geostrophic wind velocity. However, the decrease of wind velocity due to the urban buildings grows quickly with the increase of geostrophic wind velocity. So, the wind velocity above the urban area in the case of strong winds is mainly determined by a dynamical factor (the resistance of urban buildings).

Many observations in the UBL confirm our numerical results. It has been suggested for several cities that there is a critical regional wind velocity (Bornstein and Johnson, 1977; Chandler, 1965). Below this value, the wind velocity increases over an urban area; above it, wind velocity decreases due to the dominant role of the dynamical or the thermal factor. For example, the critical value of rural wind velocity is found in the works mentioned above to be in the range 3.5–5.5 m s^{-1} for London and 3.8 m s^{-1} for New York. In recent work of Karlsson (1981) that value is about 3 m s^{-1} for Uppsala.

Figure 13 shows the vertical and horizontal distributions of urban-rural temperature difference isolines. Figure 13a is for urban heating only and Figure 13b shows the additional effect of building resistance. In the first case, the top of the 0.1 K isoline is near 200 m; in the second case, it reaches 350 m. In the horizontal plane, the urban heat island expands in the direction of the wind in the second case but has similar shape.

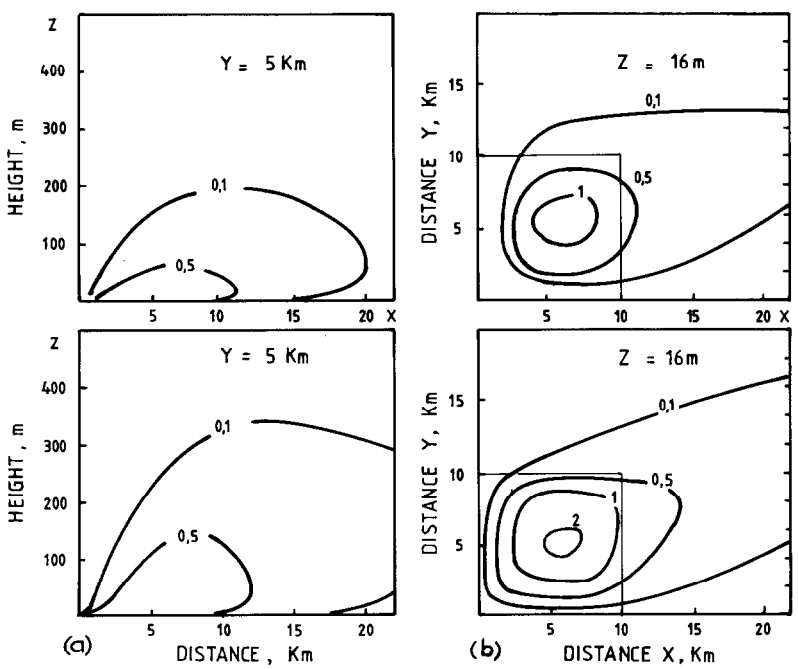

Fig. 13. Vertical and horizontal distribution of urban-rural temperature deviations (K). (a) the effect of the urban heat island ($h_b = 0$, $\theta' \neq 0$); (b) the effect of buildings and the heat island ($h_b \neq 0$, $\theta' \neq 0$).

4. Conclusions

The purpose of our work was to isolate and study the influences of particular factors on the urban atmospheric state. Our goal has been attained succesfully and our results are in qualitative agreement with observations.

Acknowledgements

We would like to thank Prof. Ulf Högström for critically reading the manuscript and suggesting numerous improvements.

Appendix A: Estimation of Building and Traffic Resistance

Mass force **F** due to building resistance can be expressed as:

$$\mathbf{F} = \frac{1}{v} cA \frac{|\mathbf{V}|\mathbf{V}}{2} = \frac{cA}{2v} |\mathbf{V}|\mathbf{V} = c_r |\mathbf{V}|\mathbf{V} \tag{A1}$$

where

$\mathbf{V}$ = wind vector,
v = the volume of urban air,
A = urban area perpendicular to wind direction,
c = resistance coefficient, equal 0.3–0.8 for obstacles in the form of rectangular parallelepipeds (Schlichting, 1974),
c_r = urban resistance coefficient.

A similar approach was used by Gavrilov (1973), Dubov and Bykova (1970) and Popov (1975) for numerical modelling of air flow in a forest canopy. We can assume that

$$c_r = \frac{cA}{2v} \sim \frac{c}{2} \frac{h\sqrt{A_b}m}{h(A_b - a_b)m} \sim \frac{c\sqrt{A_b}}{2(A_b - a_b)} \sim 10^{-3}\text{–}10^{-2} \tag{A2}$$

where

A_b = urban area divided by number of buildings (thousands m^2),
a_b = average area occupied by one building (hundreds m^2),
h = average building height (tens m),
m = number of buildings.

From (A2) we have that $c_r \sim 10^{-3}$–10^{-2} (Table II).

Similarly the kinetic energy generation by traffic in the urban area can be evaluated as

$$E_c = \frac{1}{v_R} c' A_s n \frac{W^2}{2} = c_s W^3 \tag{A3}$$

v_R = air volume in the traffic layer,
c' = nondimensional resistance coefficient (c' = 0.42–0.76, Schlichting, 1974),
n = number of moving cars in the urban area (some thousands),

TABLE II

Estimation of resistance coefficient c_r for different towns

City	h_b [m]	a_b [m^2]	A_b [m^2]	c_r [m^{-1}]
Chicago	40	1200	16000	0.0030
Madison	15	600	6900	0.0048
Frankfurt	30	600	12000	0.0034
		Average	0.0037	

W = average speed of cars (some tens km h^{-1}),
A_s = frontal area of a car,
c_s = traffic resistance coefficient.
We assume that

$$c_s = \frac{c'}{2\,v_R} A_s n = \frac{c' d_s h_s n}{2Ah_s} = \frac{c' d_s n}{2A} \tag{A4}$$

where
d_s = average width of cars (order 1 m),
h_s = average height of cars (order 1 m),
A = urban area (some hundred km^2).
Estimation of E_c on the basis of (A3), (A4) gives values in the interval 10^{-3} to 10^{0} m^2 s^{-3} (Table III).

TABLE III

Estimation of turbulent energy generation by urban traffic for different Polish towns (d_s = 2.5 m, W = 15 m s^{-1}, c' = 0.6)

City	Area [km^2]	Number of registered vehicles	Turbulent energy generation			
			Number of moving vehicles			
			1%	10%	25%	100%
Warszawa	446	137000	0.0078	0.078	0.195	0.78
Kraków	322	58500	0.0046	0.046	0.115	0.46
Poznań	228	72800	0.081	0.081	0.203	0.81
Wroclaw	293	53200	0.0046	0.046	0.115	0.46
Lódź	214	65600	0.0078	0.078	0.195	0.78
		Average	0.0066	0.066	0.165	0.66

Appendix B: Derivation of an Expression for K

The steady-state turbulent energy equation can be written:

$$K\left|\frac{\mathrm{d}\mathbf{V}}{\mathrm{d}z}\right|^2 - K\beta\frac{\mathrm{d}\theta}{\mathrm{d}z} + \mathrm{diff} = c_0\frac{b^2}{K} \tag{B1}$$

where
diff = turbulent energy diffusion terms,
c_0 = constant coefficient,
b = turbulent energy,
β = buoyancy parameter.
From the additional assumption that:

$$K = c_0^{1/4} l \sqrt{b} \tag{B2}$$

and from Equation (B1), in which for simplification, diffusion terms were neglected, we obtain the well-known formula:

$$K = l^2 \sqrt{\left|\frac{\mathrm{d}\mathbf{V}}{\mathrm{d}z}\right|^2 - \beta \frac{\mathrm{d}\theta}{\mathrm{d}z}}. \tag{B3}$$

In the case of air flow over an urban area, the turbulent energy equation should be extended to include terms describing energy generation by obstacles in the building layer and energy generation by urban traffic in the layer where cars move.

For an urban area, Equation (B1) can be modified by including the effect of turbulent energy generation in the urban area E:

$$K \left|\frac{\mathrm{d}\mathbf{V}}{\mathrm{d}z}\right|^2 + E - K\beta \frac{\mathrm{d}\theta}{\mathrm{d}z} + \mathrm{diff} = c_0 \frac{b^2}{K}. \tag{B4}$$

Neglecting diffusion terms and with the help of Equation (B2), Equation (B4) can be rewritten in the form

$$l^4 \left[K \left|\frac{\mathrm{d}\mathbf{V}}{\mathrm{d}z}\right|^2 + E - K\beta \frac{\mathrm{d}\theta}{\mathrm{d}z} \right] = K^3. \tag{B5}$$

Equation (B5) can be solved iteratively.

Substituting (B3) as a first approximation into the left side of Equation (B5), we obtain in the first iteration:

$$K = \sqrt{l^6 \left(\left|\frac{\mathrm{d}\mathbf{V}}{\mathrm{d}z}\right|^2 - \beta \frac{\mathrm{d}\theta}{\mathrm{d}z} I_\theta \right)^{3/2} + l^4 E}. \tag{B6}$$

Function I_θ ensures that the term under the root is positive. Notice that Equation (B5) is identical to (B3) when $E = 0$, $I_\theta = 1$.

References

Atwater, M. A.: 1971, 'Radiative Effects of Pollutants in the Atmosphere Boundary Layer', *J. Atm. Sci.* **28**, 1367–1373.

Blackadar, A. K.: 1962, 'The Vertical Distribution of Wind and Turbulent Exchange in Neutral Atmosphere', *J. Geophys. Res.* **67**, 3095–3102.

Bornstein, R. D.: 1968, 'Observation of the Urban Heat Island in New York City', *J. Appl. Meteorol.* **7**, 575–582.

Bornstein, R. D. and Johnson, D. S.: 1977, 'Urban-Rural Wind Velocity Differences', *Atmos. Env.* **14**, 597–604.
Bowne, N. E. and Ball, J. T.: 1970, 'Observational Comparison of Rural and Urban Boundary Layer Turbulence', *J. Appl. Meteorol.* **9**, 862–873.
Chandler, T. J.: 1965, *Climate of London*, W. Heffer and Sons, Cambridge.
Chandler, T. J.: 1968, *Selected Bibliography on Urban Climate*, WMO Publ. No. 276.
Chandler, T. J.: 1970, *Urban Climatology – Inventory and Prospect*, WMO Tech. Note No. 188.
Chandler, T. J.: 1976, *Urban Climatology and Its Relevance to Urban Design*, WMO Tech. Note No. 149.
Clarke, J. F.: 1969, 'Nocturnal Urban Boundary Layer over Cincinnati, Ohio', *Mont. Weather Rev.* **97**, 582–589.
Clarke, T. F. and McElroy, F. G.: 1970, 'Experimental Studies of Nocturnal Urban Boundary Layer', WMO Tech. Note No. 108.
De Luisi, J. J.: 1967, 'The Effects of Haze Upon Umkehr Measurements', Sci. Rep. No. 3, Dept. Met. Florida St. Univ. Tallahassee, Ph.D. Thesis.
Dirks, R. A.: 1974, 'Urban Atmosphere: Warm Dry Envelope over St. Louis', *J. Geophys. Res.* **79**, 3473–3475.
Dubov, A. S. and Bykova, L. P.: 1970, 'On Air Turbulent Characteristics Changes in Forest Canopy', *Tr. G.G.O.* **226**, 45–56 (in Russian).
Estoque, M. A. and Bhumralhar, Ch. M.: 1970, 'A Method for Solving the Planetary Boundary-Layer Equations', *Boundary-Layer Meteorol.* **1**, 169–194.
Gavrilov, A. S.: 1973, 'Structure of the Atmospheric Boundary Layer over Surface with Arbitrary Roughness Properties', *Meteorolog. i Gidrolog.* **12**, 35–42.
Graham, I. R.: 1968, 'An Aanalysis of Turbulence Statistics at Fort Wayne, Indiana', *J. Appl. Meteorol.* **7**, 90–93.
Högström, U.: 1978, *Meteorology of Cities as Related to Air Pollution Dispersion*, Proc. of WMO Symp. on Boundary Layer Physics Applied to Specific Problems of Air Pollution.
Karlsson, S.: 1981, *Analysis of Wind Profile Data from an Urban-Rural Interface Site*, Reports No. 58, Department of Meteorology, University of Uppsala.
Landsberg, H. E.: 1956, *The Climate of Towns. Int. Symp. on Man's Role in Changing the Face of the Earth*, Proc. University of Chicago Press, 584–606.
Lazareva, N. A., Orlenko, L. P., and Shklyarevich, O. B.: 1975, 'Influence of Surface Meso-nonhomogenity on Wind Profile in Atmospheric Boundary Layer', *Trudy Glav. Geof. Observ.* **362**, 102–108 (in Russian).
Oke, T. R.: 1974, *Review of Urban Climatology*, 1968–1973, WMO Techn. Note No. 134.
Oke, T. R.: 1978, *Boundary Layer Climates*, Methuen, London.
Oke, T. R. and Hannell, F. G.: 1970, *The Form of the Urban Heat Island in Hamilton, Canada*, WMO Techn. Note No. 108, 113–126.
Oke, T. R. and East, C.: 1971, 'The Urban Boundary Layer in Montreal', *Boundary-Layer Meteorol.* **1**, 411–437.
Oke, T. R. and Maxwell, G. B.: 1975, 'Urban Heat Island Dynamics in Montreal and Vancouver', *Atmos. Envir.* **9**, 191–200.
Popov, A. M.: 1975, 'Modelling of the Planetary Boundary Layer of Atmosphere in the Roughness Layer', *Bull. (Izv.) Acad. Sci. U.S.S.R. Atmospheric and Oceanic Physics* **11**, 354–358.
Pandolfo, J. P. and Jacobs, C. A.: 1973, *Tests of an Urban Meteorological-Pollutant Model Using CO Validation Data in Los Angeles Metropolitan Area*, Rpt. No. EPA-R4-73-025a. Met. Lab. Envir. Res. Cent. North-Carolina.
Schlichting, H.: 1968, *Boundary-Layer Theory*, McGraw-Hill Book Company.
Sharon, S. W.: 1965, 'A Study of Heat Transfer Coefficients in the Lowest 400 m Atmosphere', *J. Geophys. Res.* **70**, 1801–1807.
Sorbjan, Z.: 1976, 'Numerical Model of Urban Boundary Layer', Ph.D. Thesis, Politechnika Warszawska, Warszawa (in Polish).
Sorbjan, Z.: 1978a, 'Numerical Simulation of Dynamic Structure of the Atmospheric Boundary Layer in Urban Areas', *Acta Geophys. Polonica*, 167–171.
Sorbjan, Z.: 1978b, 'Numerical Simulation of Thermal Structure of Urban Boundary Layer', *Zeitschrift für Meteorol.*, 65–70 (in Russian).
Spangler, T. C., Dirks, R. A.: 1974, 'Meso-Scale Variations of the Urban Mixing Height', *Boundary-Layer Meteorol.* **6**, 423–441.

Taesler, R.: 1978, *Observational Studies of Three-Dimensional Temperature and Wind Fields in Uppsala*, Proc. of WMO Symp. on the Boundary Layer Physics Applied to Specific Problems of Air Pollution.

Taylor, P. A. and Delage, Y.: 1971, 'A Note on Finite-Difference Schemes for Surface and Planetary Boundary Layers', *Boundary-Layer Meteorol.* **2**, 108–121.

Uliasz, M.: 1979, 'Urban Effect on the Dynamics of Atmospheric Boundary Layer', *Przegl. Geofiz.* **1**, 57–64 (in Polish).